Adsorption of Dye Over Lignin Obtained from Wastewater Separation

Pummarin Khamdahsag[1], Thitisuda Jarichanon[2], Jakkapop Phanthasri[2],
Suttikorn Suwannatrai[2], Bhuckchanya Pangkumhang[3] and Visanu Tanboonchuy[2,4,5]*

[1]Environmental Research Institute, Chulalongkorn University, Bangkok, Thailand
[2]Department of Environmental Engineering, Faculty of Engineering, Khon Kaen University, Khon Kaen, Thailand
[3]Chronic Kidney Disease Preventing in the Northeast of Thailand (CKDNET), Faculty of Medicine, Khon Kaen University, Khon Kaen, Thailand
[4]Research Center for Environmental and Hazardous Substance Management (EHSM), Khon Kaen University, Khon Kaen, Thailand
[5]Research Program on Development of Appropriate Technologies for Coloring Agent Removal from Textile Dyeing, Pulp & Paper, and Sugar Industries for Sustainable Management, Center of Excellence on Hazardous Substance Management (HSM), Chulalongkorn University, Bangkok, Thailand.

Abstract

Lignin is a major by-product problem for the pulp and paper industry. In our previous work, lignin was successfully separated from alkali lignin wastewater using iron (III) trimesic (Fe-BTC). This separation resulted in three layers: supernatant, lignin sludge, and Fe-BTC powder. In this study, the lignin separated by Fe-BTC (LSF) was expected to be used as an adsorbent for reactive red-120 dye (RR-120) removal. The LSF morphology was characterized by scanning electron microscope and energy dispersive X-ray spectrometer (SEM-EDS), the specific surface area was analyzed by Brunauer-Emmett-Teller (BET) method, and the functional groups were investigated by Fourier transform infrared (FTIR) spectrometer. The removal performance of LSF over RR-120 was approximately 35% in 60 min. The maximum adsorption capacity of LSF for RR-120 was found to be 10.363 mg/g. The adsorption kinetic of RR-120 removal fitted well with the pseudo-second-order kinetic model. The adsorption isotherm model of LSF also fitted with the Langmuir isotherm model. This research suggests the high potential of LSF as a lignin-based adsorbent agent for RR-120 removal in water.

*Corresponding author: Tel.: +664-336-2140 Fax: +664-320-2571
E-mail: visanu@kku.ac.th

1. Introduction

Dyes are commonly used in industry, and in particular the textile industry consumes a large amount of water and discharges dyes as its main pollutant. These dyes are predominantly organic compounds that are difficult to be degraded and have strong toxicity. Therefore, when the dyes enter the environment, they may accumulate in some aquatic organisms [1]. Generally, synthetic dyes are divided into acidic, reactive, direct, basic, and other groups. Although different dyes are used in industries, azo and reactive classes are by far the most commonly used dyes [2]. Reactive dyes are typically azo-based chromophores combined with different types of reactive groups such as vinyl sulfone, chlorotriazine, trichloropyrimidine, and difluorochloropyrimidine [1]. Therefore, these dyes must be removed from industrial wastewater before discharging into recipient waters. Among the reactive dyes in the textile industry, reactive red-120 (RR-120) is one of the often-used dyes being hardly biodegradable associated with having aromatic rings in its structure [3]. Therefore, it must be removed from industrial wastewater before the wastewater is discharged into receiving waters.

There are several treatment technologies such as ion-exchange, adsorption, chemical precipitation, membrane filtration, flocculation, coagulation, and electrochemical methods that have been employed to treat dye-contaminated effluents [4]. Of these techniques, adsorption is one of the most common processes used in water and wastewater treatment. It is more productive in terms of economy, design and operation, and high efficiency. Mostly, adsorption is reversible because of the weak Van der Waals bonds between adsorbent and adsorbate [5].

Currently, novel materials are being investigated for their adsorptive potentiality, which obtain from agriculture by-products, industrial by-products, industrial waste biomass, and natural materials. In this study, a by-product from pulp and paper industry or lignin was tested for use as an adsorbent due to its primary properties: accessibility, high porosity, and high specific surface, which are characteristics that point to it being very beneficial in adsorption process [6].

Special attention was paid to lignin obtained from a pulp and paper wastewater treatment by iron (III) trimesic (Fe-BTC), which was used as coagulant-flocculant in a former study by our team [7]. After the treatment, three layers including supernatant, alkaline lignin sludge, and Fe-BTC powder occurred, and were simply separated [7]. Typically, in the pulp and paper industry, lignin is burned and used as not only a fuel source but also as an added value adsorbents because of its its high porosity and specific surface area [8]. Moreover, lignin has a variety of functional groups that give it the necessary characteristics to be an adsorbent [9, 10].

This research aimed to investigate the utilization of alkaline lignin separated with Fe-BTC (LSF) for use as an RR-120 adsorption. Experiments with various operating parameters such as RR-120 initial concentration and contact time of RR-120 adsorption were conducted. The adsorption kinetics and adsorption isotherm results were used to estimate the potential of LSF as an adsorbent agent for RR-120 removal.

2. Materials and Methods

2.1 Materials

Alkaline lignin (CAS no.: 8068-05-1) was purchased from Tokyo Chemical Industry CO., LTD. Ferric chloride hexahydrate ($FeCl_3.6H_2O$) was a QRëC New Zealand product. Benzene-1,3,5-tricarboxylic acid (H_3BTC) was purchased from Sigma-Aldrich. Ethanol was purchased from RCI Labscan. RR-120 was an analytical grade. Deionized (DI) water and reverse osmosis (RO) water were lab grade.

2.2 Lignin adsorbent and wastewater preparation

2.2.1 Adsorbent preparation

LSF as an adsorbent was obtained from wastewater via a coagulation process using Fe-BTC as coagulant-flocculant following our previous report [7]. As shown in Figure 1, Fe-BTC powder and LSF sludge settled separately; Fe-BTC at the bottom, LSF in the middle, and clear supernatant at the top. Then, LSF and Fe-BTC powder were separated by centrifuge and washed with RO water for several times. Next, LSF was dried in a hot air oven at 103 °C for 24 h. The dark-brown powder was collected and kept in a desiccator.
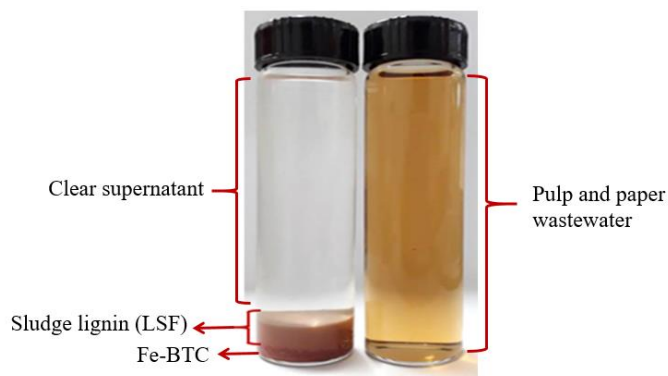

Figure 1. Separation of wastewater into layers: Fe-BTC powder at the bottom, LSF in the middle, and clear supernatant at the top

2.2.2 Wastewater preparation

The stock of synthetically colored wastewater was prepared by dissolving RR-120 in RO water. Likewise, the synthetic wastewater was prepared by dissolving LSF in DI water.

2.3 Characterization

The morphology of the LSF was recorded using a scanning electron microscopy and energy dispersive X-ray spectrometer (SEM-EDS) (LEO, 1450 VP) with a magnification of 5000x. A BET surface area pore size and pore volume distribution analyzer (BEL-Japan, BELSORP-mini II) was used to measure the specific surface area, pore-volume, and pore diameter of LSF. The degassing temperature was set at 150 °C. The functional groups of the LSF samples were investigated by Fourier transform infrared (FTIR) spectrometer (Bruker, TENSOR27) using the KBr pellet method and scanning over the range of 400 and 4000 cm^{-1}. The characteristics of LSF were compared to those of pristine alkaline lignin (PAL).

2.4 Adsorption kinetic models

The adsorption kinetic was conducted in a beaker with magnetic stirring to complete mixing at room temperature (30±1°C) in order to find the most suitable contact time. Based on the preliminary study, the adsorption kinetic was performed at the most suitable experimental conditions: an RR-120 initial concentration of 10 mg/l for 1 l, pH 6.5, and LSF dosage of 0.5 g/l. The sampling follows the

predetermined time until suitable contact time, and these samples were filtered using 0.45 μm-pore-size PTFE filters. The concentrations of the sample were analyzed by UV-vis spectrophotometer (HACH, DR 6000) under a maximum wavelength of 536 nm. The removal efficiency (R) and adsorption capacity of RR-120 (Q_e, mg of dye/g of adsorption) were calculated using the Equations (1) and (2) below,

$$R(\%) = \frac{C_0 - C_e}{C_0} \times 100 \tag{1}$$

$$Q_e = \frac{C_0 - C_e}{W} \times V \tag{2}$$

where C_0 is the initial concentration (mg/l); C_e is the final concentration (mg/l); W is the mass of LSF (g); and V is the volume of RR-120 solution (l).

Adsorption kinetic models were proposed to understand the mechanism and to scale-up the efficiency of adsorption. To investigate the potential rate-determining step such as pseudo-first-order and pseudo-second-order kinetic models, the experimental data were tested. The linear form of the pseudo-first-order and pseudo-second-order models are given by the Equations (3) and (4),

$$\ln(q_e - q_t) = \ln q_e - k_1 t \tag{3}$$

$$\frac{t}{q_t} = \frac{1}{k_2 q_e^2} + \frac{t}{q_e} \tag{4}$$

where q_e and q_t are the amounts of RR-120 adsorbed by LSF at equilibrium and at various time t (mg/g); k_1 is the equilibrium rate constant of pseudo-first-order kinetics (min^{-1}); t is the contact time (min); k_2 is the equilibrium rate constant of the pseudo-second-order kinetics (g/mg-min) [11].

2.5 Adsorption isotherm models

Adsorption isotherms were conducted at different RR-120 initial concentrations from 0.5 to 30 mg/l at room temperature (30 ± 1 °C) for 60 min. In this process, the concentrations of RR-120 in the solution were always determined with a UV-Vis spectrophotometer (HACH, DR 6000) under a maximum wavelength of 536 nm. The analysis of equilibrium data by fitting to different isotherm models is important in the estimation of practical adsorption capacity and optimization of adsorption system design. The results from the study were therefore calculated using two models including Langmuir and Freundlich adsorption isotherm models, which are the most commonly used theoretical models. The models can be expressed by the Equations (5) and (6),

$$\text{Langmuir}; \quad Q_e = \frac{Q_m K_L C_e}{1 + K_L C_e} \tag{5}$$

$$\text{Freundlich}; \quad Q_e = K_F C_e^{1/n} \tag{6}$$

where C_e is the RR-120 equilibrium concentration (mg/l) and Q_e is the adsorption amount of RR-120 after adsorption equilibrium (mg/g). Q_m is the theoretical saturated adsorption capacity (mg/g) and K_L is a Langmuir constant representing the affinity of adsorbate and adsorbent (l/mg). K_F is a

Freundlich constant indication of the relative adsorption capacity of adsorbent (mg/g) and 1/n is the adsorption intensity [12].

3. Results and Discussion

3.1 Characteristics of LSF

The morphologies of PAL and LSF from the SEM analysis technique is shown in Figure 2. PAL showed large particles with bare smooth surfaces, while LSF presented small fragments on the smooth surface of bulk particles. The semi-quantitative elemental results of PAL and LSF obtained from SEM-EDS analysis are presented in Table 1. The elements resulting in LSF held Fe about 5.74% whereas there was no Fe presented on PAL.
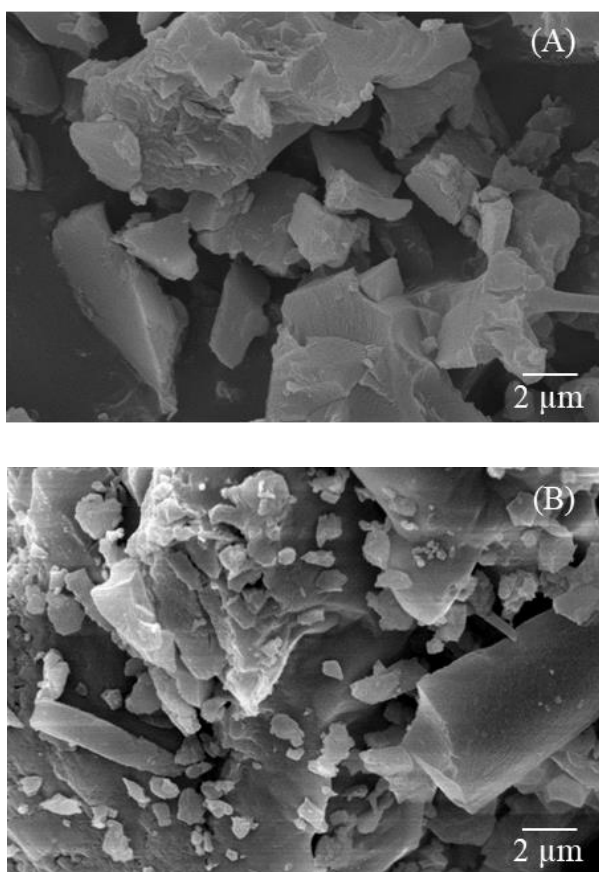

Figure 2. SEM images of (A) pristine alkaline lignin (PAL) and (B) lignin separated by Fe-BTC (LSF)

Table 1. Semi-quantitative elemental results of PAL and LSF obtained from SEM-EDS

	Weight (%)						
	C	**O**	**Na**	**Mo**	**Fe**	**Others**	**Total**
PAL	66.35	24.46	5.32	3.87	-	-	100
LSF	63.88	17.43	5.36	1.78	5.74	5.81	100

The specific surface area from the BET method (S_{BET}), total pore volume (V_p), and pore diameter (d_p) of PAL and LSF are shown in Table 2. The S_{BET} of LSF was found at 3.71 m²/g and that was 3.37 times higher than that of PAL (1.10 m²/g). The low value of PAL S_{BET} supported the interpretation of the material roughness observed from SEM. An increase in LSF S_{BET} could be related to the small fragments. The increase of LSF S_{BET} is supposed to be beneficial for an adsorbent. The total pore volume (V_p) of LSF was more than PAL, and the average pore size of LSF was also increased. Besides, the d_p of LSF (29.44 nm) is classified as a mesoporous material as recommended by IUPAC.

Table 2. Specific surface area from the BET method (S_{BET}), total pore volume (V_p), and pore diameter (d_p) of PAL and LSF

	S_{BET} (m²/g)	V_p (cm³/g)	d_p (nm)
PAL	1.10	0.01	17.00
LSF	3.71	0.02	29.44

FTIR spectra were recorded to identify functional groups in the lignin. The FTIR peaks of PAL and LSF are shown in Figure 3. The C-H stretching peaks at 2944 and 2842 cm⁻¹ appeared only on the PAL as well as guaiacyl lignin units of C-C, C-O, C=O at 1604, 1127, and 823 cm⁻¹, respectively. The nitro compound stretching at 1523 cm⁻¹ was also observed for the PAL. For LSF, the peak at 1706 cm⁻¹ on LSF was interpreted as carboxylic acid. The LSF FTIR peak of 1625 to 700 cm⁻¹ seemed to be the combination of FTIR from Fe-BTC and lignin [7]. The C=O bond at 1625 cm⁻¹, SO_3 groups stretching at 1042 cm⁻¹, C-O bond at 1381, 1220, and 1050 cm⁻¹, and C-H bond at 762 and 700 cm⁻¹ were observed for LSF. The Fe-O at 611 and 478 cm⁻¹ were also shown which were due to the Fe releasing from unsaturated sites of Fe-BTC [6, 13, 14]. The existence of Fe-O was associated with the results from SEM-EDS. Therefore, there was a good possibility to utilize the LSF as RR-120 adsorbent compared to the PAL.
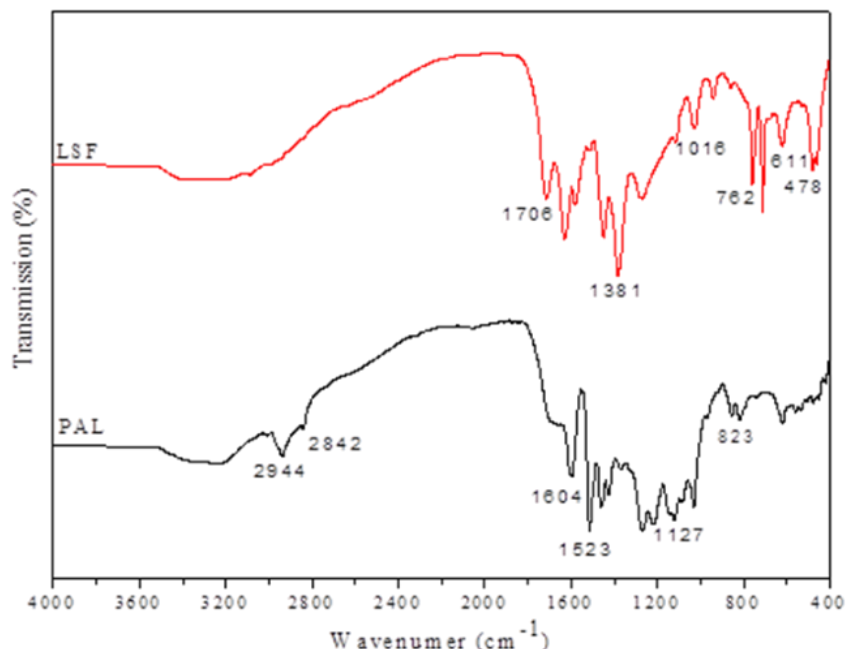
Figure 3. FTIR spectra of pristine alkaline lignin (PAL) and lignin separated by Fe-BTC (LSF)

3.2 Adsorption kinetics

The effect of contact time on the adsorption of RR-120 at room temperature ($30 \pm 1°C$) by LSF was done under the RR-120 initial concentration of 10 mg/l, pH of 6.5, and LSF dosage of 0.5 g/l, as presented in Figure 4. It was found that approximately 35% of the equilibrium adsorption capacity for RR-120 occurred within 60 min. The adsorption ability of LSF is probably due to the Fe-O remaining in the LSF structure. The blank tests of LSF in DI water and RR-120 in RO water for interference and photolysis-volatilization, respectively, were found insignificantly.

To investigate the adsorption kinetics, pseudo-first-order and pseudo-second-order models were applied. Table 3 summarizes the calculated parameters of kinetic modeling. Based on the R^2 value, the kinetic of RR-120 adsorption fitted well with a pseudo-second-order model. This implies that the adsorption kinetic follows the pseudo-second-order rate mechanism with higher values of correlation coefficient ($R^2 = 0.983$), q_2 of 4.919 mg/g, and k^2 of 0.047 g/mg-min. Besides, this model assumes the rate-limiting step of adsorption as chemisorption between the molecules of RR-120 and the active sites of the LSF [15].
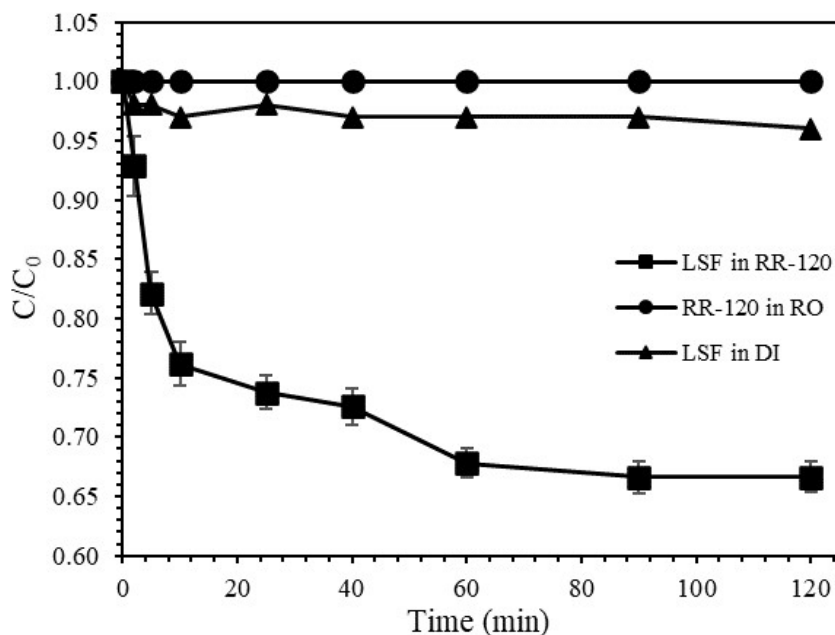
Figure 4. Effect of contact time on the adsorption of RR-120 on LSF

Table 3. Kinetic parameters of the pseudo-first-order and pseudo-second-order kinetic models for the adsorption of RR-120 on LSF

Pseudo-first-order	q_1 (mg/g)	k_1 (min^{-1})	R^2
	3.155	0.124	0.928
Pseudo-second-order	q_2 (mg/g)	k_2 (g/mg-min)	R^2
	4.919	0.047	0.983

3.3 Adsorption isotherm

The adsorption isotherms describe the distribution of adsorbate species between the liquid phase when the adsorption process reaches an equilibrium state. To obtain the adsorption capacity of LSF for RR-120, the experimental conditions were under pH 6.5, LSF dosage of 0.1 g/l, room temperature (30±1°C), and contact time of 60 min. The maximum adsorption capacity (Q_m) of RR-120 on LSF was found at 10.363 mg/g as presented in Table 4. In Figure 5, the higher correlation coefficient of the Langmuir isotherm model ($R^2 = 0.965$) means that the behavior adsorption RR-120 by LSF matched the isotherm which describes the homogeneous system. Moreover, the adsorption can be characterized as monolayer adsorption, and the adsorption equilibrium is steady-state [16].

Table 4. Langmuir and Freundlich isotherm model parameters for the adsorption of RR-120 on LSF

Langmuir isotherm	Q_m (mg/g)	K_L (L/mg)	R^2
	10.363	0.065	0.965
Freundlich isotherm	K_F (mg/g)	n	R^2
	1.015	1.695	0.938
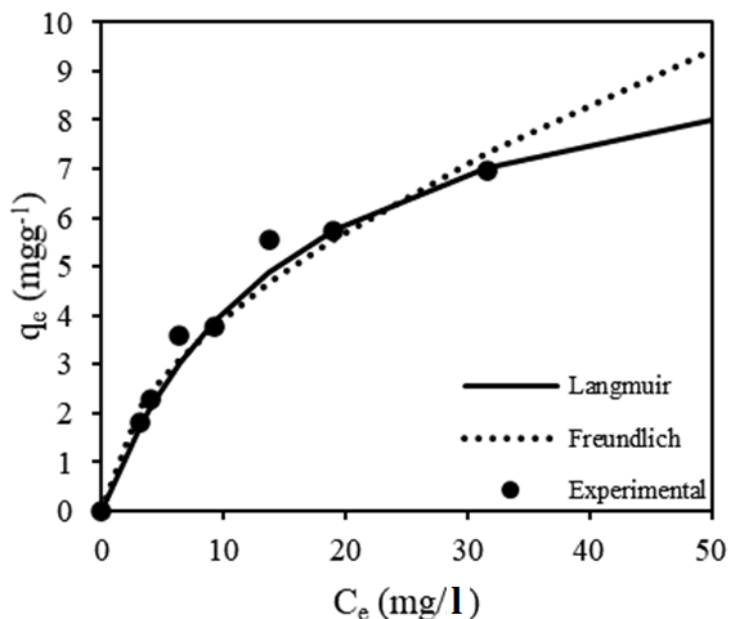
Figure 5. Adsorption isotherms of RR-120 onto LSF

4. Conclusions

LSF was used as an adsorbent for RR-120 removal and proved to be superior to PAL. The results showed that the adsorbent could effectively adsorb RR-120 dye. The adsorption kinetic of RR-120 fitted well with the pseudo-second-order kinetic model. The adsorption isotherm followed the Langmuir isotherm model. The overall result indicated the potential use of LSF as an adsorbent for adsorption of RR-120. There is an opportunity for further study to increase the specific surface area of LSF further promoting the utilization of LSF. It is expected to enhance the adsorption capacity of RR-120 as well as other dyes over the modified LSF.

5. Acknowledgements

References

[1] Bazrafshan, E., Ahmadabadi, M. and Mahvi, A.H., 2013. Reactive red-120 removal by activated carbon obtained from cumin herb wastes. *Fresenius Environmental Bulletin,* 22(2A), 584-590.

[2] Hossein, M.A. and Behzad, H., 2012. Removal of reactive red 120 and direct red 81 dyes from aqueous solutions by Pumice. *Research Journal of Chemistry and Environment,* 16(1), 62-68.

[3] Amran, M., Salleh, M., Khalid, D., Azlina, W., Abdul, W. and Idris, A., 2011. Cationic and anionic dye adsorption by agricultural solid wastes: A comprehensive review. *Desalination,* 280, 1-13.

[4] Leah, M.F., Love, M., Angela, D., Ruffel, R., Paoprasert, P. and Daniel, M., 2018. Adsorption of methylene blue dye and Cu (II) ions on EDTA-modified bentonite: Isotherm, kinetic and thermodynamic studies. *Sustainable Environment Research,* 28(5), 1-9.

[5] Kaykhaii, M., Sasani, M. and Marghzari, S., 2018. Removal of dyes from the environment by adsorption process. *Chemical and Materials Engineering,* 6(2), 31-35.

[6] Suteu, D., Malutan, T. and Bilba, D., 2010. Removal of reactive dye Brilliant Red HE-3B from aqueous solutions by industrial lignin: Equilibrium and kinetics modelling. *Desalination,* 255(1-3), 84-90.

[7] Pangkumhang, B., Jutaporn, P., Sorachoti, K., Khamdahsag, P. and Tanboonchuy, V., 2019. Applicability of iron (III) trimesic (Fe-BTC) to enhance lignin separation from pulp and paper wastewater. *Sains Malaysiana,* 48(1), 199-208.

[8] Feizi, Z.H. and Fatehi, P., 2018. Production of flocculants, adsorbents, and dispersants from lignin. *Molecules,* 23, 868-893.

[9] Tesfaw, B., Chekol, F., Mehretie, S. and Admassie, S., 2016. Adsorption of Pb (II) ions from aqueous solution using lignin from Hagenia abyssinica. *Bulletin of the Chemical Society of Ethiopia,* 30(3), 473-484.

[10] Xu, T., Zhang, N., Nichols, H.L., Shi, D. and Wen, X., 2007. Modification of nanostructured materials for biomedical applications. *Materials Science and Engineering: C,* 27(3), 579-594.

[11] Kajjumba, G.W., Emik, S., Özcan, A., Özcan, H.K. and Öngen, A., 2018. Modelling of adsorption kinetic processes-errors, theory and application. *Intech,* 1, 13, https://doi.org.10.5772/intechopen.80495

[12] Ali, I.H., Mesfer, M.K.A., Khan, M.I., Danish, M. and Alghamdi, M.M., 2019. Exploring adsorption process of lead (II) and chromium (VI) ions from aqueous solutions on acid activated carbon prepared from *Juniperus procera* leaves. *Processes,* 7(4), 217, https://doi.org/10.3390/pr7040217

[13] Kanna, R.R., Lenin, N., Sakthipandi, K. and Kumar, A.S., 2018. Structural, optical, dielectric and magnetic studies of gadolinium-added Mn-Cu nanoferrites. *Journal of Magnetism and Magnetic Materials,* 453, 78-90.

[14] Kerolli-Mustafa, M., Bačič, I. and Ćurkovič, L., 2013. Investigation of jarosite process tailing waste by means of raman and infrared spectroscopy. *Materialwissenschaft und Werkstofftechnik,* 44(9), 768-773.

[15] Li, Z., Xiao, D., Ge, Y. and Koehler, S., 2015. Surface-functionalized porous lignin for fast and efficient lead removal from aqueous solution. *Applied Materials & Interfaces,* 7(27), 15000-15009.
[16] Ge, Y., Qin, L. and Li, Z., 2016. Lignin microspheres: An effective and recyclable natural polymer-based adsorbent for lead ion removal. *Materials and Design,* 95, 141-147.